Research Article

Nano Biomed Eng

Zwitterionic Surfactant Modified Carbon Nanotubes Incorporated Percolative Polymer Composites with Improved Features

Farrukh Bashir[1,2,§], Tajamal Hussain[1,§], Adnan Mujahid[1], Ayesha Mushtaq[2✉], Muhammad Aamir Raza[3], Mirza Nadeem Ahmad[4], Muhammad Zahid[5], Muhammad Imran Din[1], Huma Tareen[2]

[1] Institute of Chemistry, University of the Punjab, Lahore, Pakistan
[2] Department of Chemistry, Sardar Bahadur Khan Women's University, Quetta, Pakistan
[3] Pakistan Council of Scientific and Industrial Research Laboratories Complex, Quetta, Pakistan
[4] Institute of Chemistry, Government College University, Faisalabad, Pakistan
[5] Department of Chemistry, University of Agriculture Faisalabad, Pakistan

[§] Farrukh Bashir and Tajamal Hussain contributed equally to this work

✉ Corresponding author. E-mail: ayeshamushtaq2000@yahoo.com

Received: Dec. 1, 2022; **Revised:** Feb. 2, 2023; **Accepted:** Apr. 14, 2023

Citation: F. Bashir, T. Hussain, A. Mujahid, et al. Zwitterionic surfactant modified carbon nanotubes incorporated percolative polymer composites with improved features. *Nano Biomedicine and Engineering*, 2023, 15(2): 136−149.

http://doi.org/10.26599/NBE.2023.9290018

Abstract

Modification of carbon nanotubes (CNTs) and their incoporation in polymer matrix have attracted much attention of researchers. As maximum dispersion of CNTs could enhance the properties of matrix dynamically, researchers are trying to find new methodologies to obtain this target. However, maximum dispersion remains a great challenge and under the stage of progress. Here, we claimed the synthesis of composites with a highly uniform dispersion of the filler that results significantly improved electrical features. In this regard, composites of polymethylmethacrylate (PMMA) were fabricated by using pristine and zwitterionic surfactant (ZIS) modified CNTs (ZIS-CNTs). Characterization was done by using ultraviolet–visible (UV–Vis), Fourier transform infrared (FTIR), X-ray diffraction (XRD), scanning electron microscopy (SEM), and thermo gravimetric analysis (TGA) techniques. UV–Vis and FTIR spectroscopy confirmed the synthesis of ZIS-CNTs and composites. UV–Vis spectra showed an increase in wavelength with the decrease in optical band gap for CNTs-based (CNTs/PMMA) and ZIS-CNTs-based (ZIS-CNTs/PMMA) composites. SEM and XRD studies confirmed a significant homogenoeus and uniform dispersion of CNTs in ZIS-CNTs/PMMA composites. An increase in conductivity of PMMA from 10^{-9} to 10^{-2} and 10^{-1} S/cm was observed on addition of less than 1% (mass fraction) of CNTs without and with modification by ZIS, respectively. Low values of percolation threshold at 0.5% and 0.005% for CNTs/PMMA and ZIS-CNTs/PMMA composites were obtained, respectively. TGA analysis showed a slow rate of decomposition for composites than that for pure PMMA. Around 600 °C, 3% CNTs/PMMA and 7% ZIS-CNTs/PMMA composites were left in the end, which depicts the increase in thermal stability of PMMA. This work depicts a better dispersion of CNTs in PMMA matrix via slight modification in synthesis as well as by using ZIS as surfactant.

Keywords: polymer composite; enhanced dispersion of carbon nanotubes (CNTs); increased electrical conductivity; low percolation threshold; improved thermal stability

Introduction

To obtain outstanding processability and versatile functionalities, researchers are trying to incorporate polymer matrix with functional nanoparticles. The addition of conducting nanoparticles into the insulating polymer matrix is under more consideration [1]. Electrical properties of such polymer composites are well explained in terms of percolation theory [2–4]. Hence, the highest conductivity and lowest percolation threshold values are the main objectives of a researcher while synthesizing polymer composites using such nano-materials as conducting filler [5]. For the development of polymer composites reinforced by nano materials, carbon nanotubes (CNTs) and graphene are found to be excellent fillers [6]. CNTs show remarkable electrical, thermal and mechanical properties along with versatile morphologies [7, 8] . These significant properties make them unique among all nanoparticles.

It is reported that the extraordinary conducting properties of CNTs have opened a new era in the field of CNTs-based nanocomposites that include electromagnetic interference shielding (EMI), chemical sensors, adsorbents, and many more [9]. However, the strong interaction between the CNTs via van der Waals forces and weak interactions between the polymer matrix and the CNTs as filler, lead to the improper dispersion and reagglomeration of the filler in the matrix. This disadvantage is found to be a crucial barrier in the practical applications of CNTs [10]. Different approaches have been applied to overcome the improper dispersion of CNTs such as their covalent [11] or noncovalent functionalization [12], polymer wrapping [13, 14], and addition of surfactants [15, 16].

In the present research, two parallel approaches have been adopted to reduce the reagglomeration of CNTs. One is the modification of CNTs by 3-(N,N-dimethyloctadecyl-ammonio) propane sulfonate, a zwitterionic surfactant (ZIS), and the other is the pre-treatment of CNTs by ultra sonication. Further, these two types of CNTs were used in the synthesis of polymer composites. Polymer used in this research was polymethylmethacrylate (PMMA). Low dielectric loss, excellent mechanical strength, and a high degree of transparency of PMMA sheets make them the best choice as a matrix for the synthesis of polymer composites [17]. Similarly, ZIS possesses unique properties, such as pH stability, high solubility, low toxicity, high surface activities, bioactivity, wide isoelectric range, and potential tendency to reduce agglomeration due to electrostatic repulsion [18]. It is also reported that modification of CNTs by ZIS results in stable dispersion [19]. Therefore, in present research CNTs were modified by ZIS in order to have a uniform dispersion in the polymer matrix. The action of ZIS, in dissembling of CNTs, is tried to be illustrated in two-step mechanism as shown in Fig. 1. ZIS contains a hydrophobic-octadecyl tail and a hydrophilic-sulfonate with a quaternary ammonium head group. First, the octadecyl tail of ZIS gets associated at the surface of CNTs via van der Waals force and the zwitterionic head group is alinged in the space. In the second step, these zwitterionic head groups, which belong to different CNTs, develop significant dipole–dipole electrostatic attractions upon approaching each other, thus helpful in the dissembling of CNTs [20].

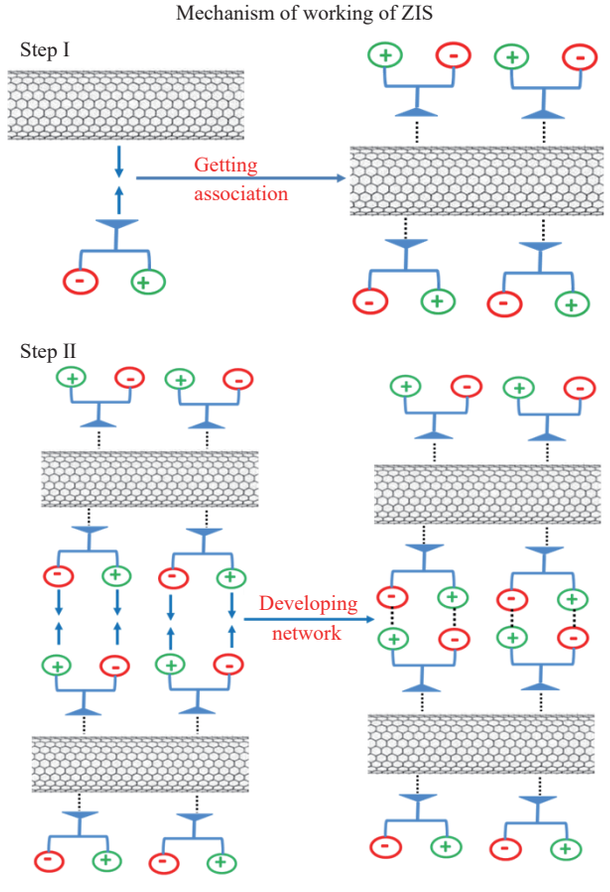

Fig. 1 Schematic representation of dissembling of CNTs with the help of zwitterionic surfactant.

Series of CNTs and ZIS-CNTs incorporated PMMA-based, CNTs/PMMA, and ZIS-CNTs/PMMA

composites, respectively, with different amounts of CNTs have been prepared. Fourier transform infrared (FTIR) and ultraviolet–visible (UV–Vis) spectrometers were used to characterize the synthesis of ZIS-CNTs and composites. Electrical parameters such as conductivity, dielectric constants, and dielectric loss for all composites were measured at different frequencies up to 1 MHz. Scanning electron microscopy (SEM) and X-ray diffraction (XRD) analysis have also been used to characterize composites for the dispersion of CNTs and ZIS-CNTs. Thermal gravimetric analysis (TGA) has been performed to check the thermal stability of the composites. With the help of techniques used to characterize composites, role of ZIS and effect of pretreatment have also been highlighted in improving the features of composites.

Experimental

Materials and methods

Multi walled carbon nanotubes (CNTs) (outer diameter × length: 6–9 nm × 5 μm; 95% purity), polymethyl methacrylate (PMMA) (average relative atomic mass: 35 000), 3-(N,N-Dimethyloctadecyl-ammonio) propanesulfonate (relative atomic mass: 419.7; 99% purity) were purchased from sigma Aldrich. Chloroform (relative atomic mass: 119.3; ≥ 99% purity) was purchased from Merck. All chemicals were used as received.

Synthesis of ZIS-CNTs as filler

An amount of 1 g of ZIS was dissolved in 200 mL of distilled water followed with the addition of same amount of CNTs in the solution and mixture was kept on stirring for 1 h. The mixture was then subjected to ultrasonication for next 1 h. The suspended solution was left for 14 h at room temperature for the maximum settling of suspended particles. Finally, solution was filtered with poly tetra fluoro ethylene (PTFE) filter paper and washed with distilled water. This residue was dried in oven at 60 °C for 14 h to have dry ZIS-CNTs [21].

Synthesis of composites

For preparation of CNTs/PMMA and ZIS-CNTs/PMMA composites, solution mixing method as given in Ref. [22] was used with slight modification. First calculated amount of CNTs, depending upon the required composition of the filler, was added in chloroform and kept on stirring for 1 h. Afterwards, the suspended mixture was ultra-sonicated additionally for next 20 min to acquire the uniform dispersion. This suspension was added in solution of PMMA and kept under ultra sonication for next 25 min. To get thin films, the suspended solution was casted on petri dish for the solvent evaporation at room temperature. Similar method was follwed for the synthesis of ZIS-CNTs/PMMA composites with different concentrations of ZIS-CNTs as filler.

Characterization

Synthesized composites were characterized by FTIR spectrophotometer (CARY-630) of Agilent in the range 650–4 000 cm^{-1} to study the interaction between the filler and the matrix. To record electronic absorbance spectra and optical properties of the pure PMMA, CNTs/PMMA, and ZIS-CNTs/PMMA composites, UV–Vis double beam spectrophotometer (PG Instrument; model: UVD-T90+) was used in the spectral range of 200–800 nm. Precision LCR meter (E4980AL) of Keysight with frequency range of 40 Hz to 1 MHz was used to measure the resistance and capacitance of the composites. XRD analysis of the PMMA and its composites was done by AXS D2 PHASER powder diffractometer of Bruker. Dispersion of filler in the polymer matrix was studied through SEM images taken by Hitachi SEM (S3700N). Effect of filler on the thermal stability of the composite was analyzed by TGA (TA Instrument; SDT-Q600) from room temperature to 600 °C, under nitrogen atmosphere at a heating rate of 20 °C/min.

Results and Discussion

FTIR and UV–Vis spectroscopy

Analysis of the FTIR spectra confirms the synthesis of ZIS-CNTs, CNTs/PMMA, and ZIS-CNTs/PMMA composites. Figure 2(a) shows the spectra of pristine PMMA, powder CNTs, and composites with 1%, 7%, and 12% (mass fraction) of CNTs, respectively. In the spectrum of powder CNTs, no infrared (IR) active species is observed, however, the band range between 2 000 and 2 200 cm^{-1} represents the imperfect carbon dioxide compensation from the atmosphere [23]. The characteristic peaks of PMMA at 1 063 to 1 270 cm^{-1} correspond to stretching vibrations of the ester bond. The peak around 1 430 cm^{-1} belongs to bending

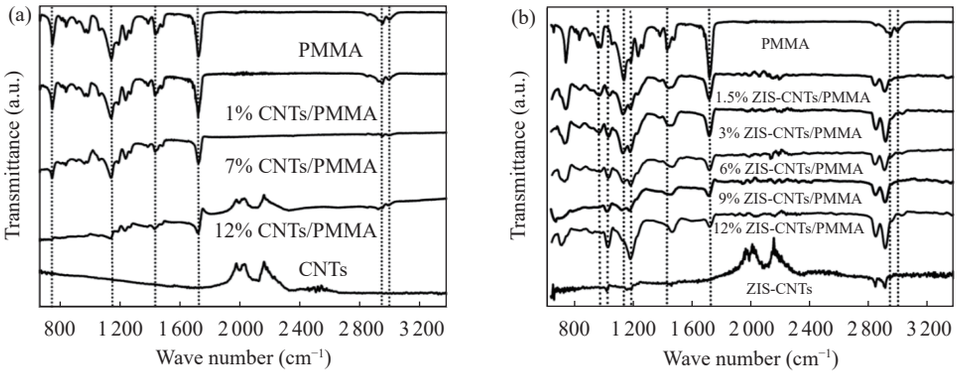

Fig. 2 FTIR spectra of **(a)** pure PMMA, CNTs, and CNTs/PMMA composites and **(b)** pure PMMA, ZIS-CNTs, and ZIS-CNTs/PMMA composites at different concentrations.

vibration of —CH bond in methyl group. Peaks at 2 953 and 3 000 cm^{-1} correspond to stretching vibrations of —CH bond in CH_2 and CH_3 groups, respectively. The peak around 1 720 cm^{-1} corresponds to carbonyl group of PMMA [24]. Reoccurrence of peak pattern of pure PMMA in all spectra of CNTs/PMMA confirms that no chemical reaction takes place between PMMA and CNTs. In FTIR spectrum of CNTs, prominent peaks are present around 2 000 cm^{-1} and appearance of peak as same position in the FTIR spectrum of CNTs-PMMA composites again confirms that no chemical reaction takes place in the synthesis of composites. Figure 2(b) represents the FTIR spectra of pure PMMA, powder of ZIS-CNTs, and ZIS-CNTs/PMMA composites at 1.5%, 3%, 6%, 9%, and 12% modified CNTs. Low intensity peaks at 2 850–2 915 cm^{-1} in the spectrum of ZIS-CNTs powder correspond to alkyl chains of ZIS, and the peak at 1 474 cm^{-1} shows the presence of sulphonic group while the peak at 1 028 cm^{-1} shows the symmetric vibration of SO_2 [25, 26]. A shift of peaks in ZIS-CNTs/PMMA composite as compared to PMMA from 1 430 to 1 474 cm^{-1} and 2 953–3 000 cm^{-1} to 2 855–2 924 cm^{-1} is due to the chains of ZIS. The appearance of characteristics peaks of ZIS-CNTs in the FTIR spectra of ZIS-CNTs/PMMA confirms the successful incorporation of ZIS-CNTs in the PMMA matrix and the pattern of characteristics peaks of PMMA remains intact in the spectrum of ZIS-CNTs/PMMA composite, which again indicates that no chemical reaction took place.

UV–Vis spectra of pure PMMA, CNTs/PMMA, and ZIS-CNTs/PMMA composites at 12% CNTs are shown in Fig. 3(a). Pure PMMA has the value of λ_{max} at 265 nm which is between the range (260–290 nm) as given in Ref. [8], while for CNTs/PMMA and ZIS-CNTs/PMMA composites, λ_{max} is observed at 274 and 270 nm, respectively. Overall, a shift in absorption band upon composite formation has been attributed to the existence of physical interaction between filler and matrix. Tauc plot, as shown in Figs. 3(b)–3(d), is used to calculate optical band gaps with the help of UV–Vis absorption studies [27]. The extraplotation of the linear portion of the plot between $(\alpha hv)^2$ vs. hv provides the value of the optical band gap. The absorption coefficient α is calculated by [26]:

$$\alpha = 2.303A/l$$

where A is the optical density (absorption) and l is the path length of the cuvette used (i.e., l = 1 cm). Table 1 gives the difference in the optical band gap with respect to pristine PMMA.

X-ray diffraction and SEM analysis

Figure 4 shows the XRD pattern of pristine PMMA and composites of CNTs/PMMA and ZIS-CNTs/PMMA. Three characteristics broad humps of PMMA were observed at 16.5°, 29.1°, and 40.86°. These values are matching well with previous study results [28, 29]. However, in the XRD pattern of the CNTs/PMMA composite, the peak pattern of PMMA reappears without any change, indicating that the structure of PMMA remains intact. Additionally, a peak at 25.6° shows up belonging to CNTs. A similar peak also shows up at the same position in the spectrum of ZIS-CNTs/PMMA composite. An interesting observation in ZIS-CNTs/PMMA composite is enhancement in sharpness of the peak around 16°. This indicates that the crystalline structure of PMMA enhances upon the addition of ZIS-CNTs, which supports the observation of tremendous improvement of electrical features of ZIS-CNTs/PMMA composites. The peak pattern in XRD of ZIS-CNTs/PMMA does not resemble well with that of PMMA as CNTs/PMMA does with PMMA,

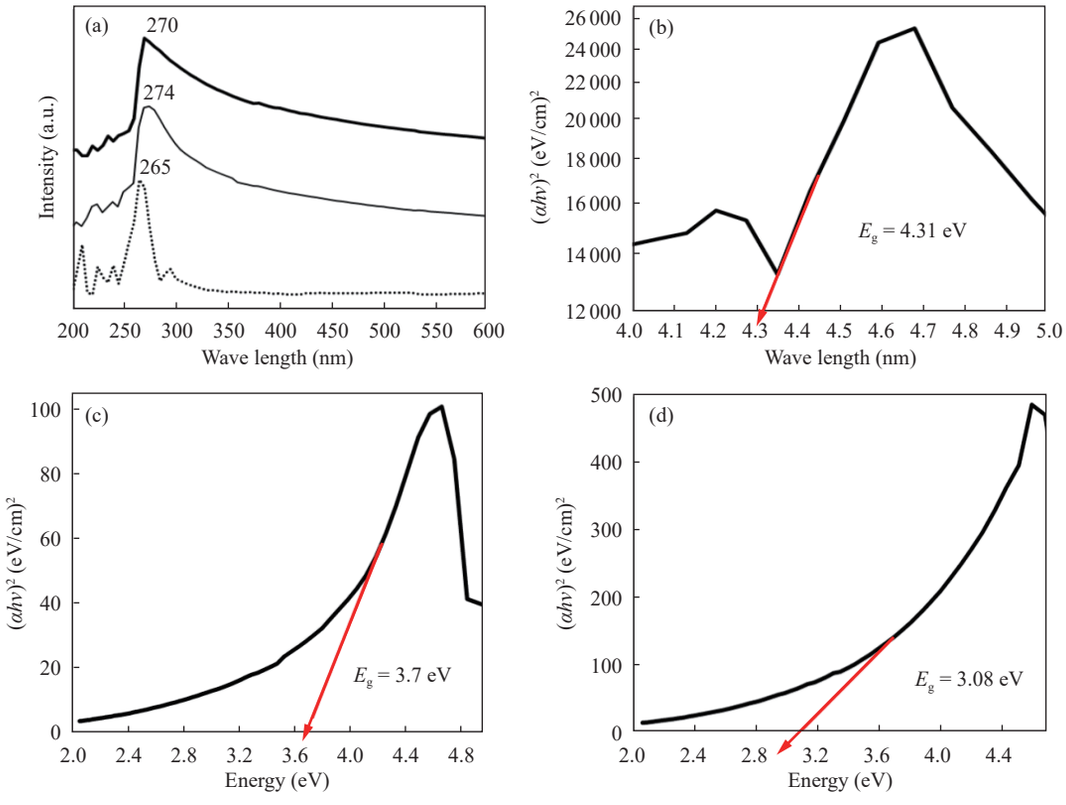

Fig. 3 (a) UV–Vis spectra with dotted, thin lined, and thick lined. Tauc plots of **(b)** pristine PMMA, **(c)** CNTs/PMMA, and **(d)** ZIS-CNTs/PMMA composites, respectively.

Table 1 Optical band gap energies of PMMA, CNTs/PMMA, and ZIS-CNTs/PMMA composites at 12% of CNTs

Sample ID	Band gap (eV)	Difference in band gap with respect to pure PMMA (eV)
PMMA	4.31	—
CNTs/PMMA	3.7	0.61
ZIS-CNTs/PMMA	3.08	1.23

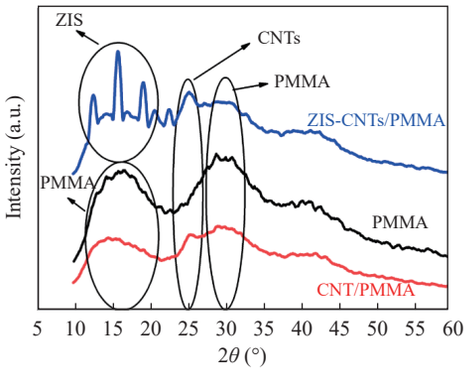

Fig. 4 XRD patterns of pristine PMMA, CNTs/PMMA, and ZIS-CNTs/PMMA composites.

which shows the considerable interaction between PMMA and ZIS-CNTs. This interaction is the main reason behind the proper dispersion of the ZIS-CNTs in PMMA. SEM images of the CNTs/PMMA and ZIS-CNTs/PMMA composites with surface profile and topography are given in Fig. 5. These images clearly depict the effect of the presence or absence of ZIS on the dispersion of CNTs in PMMA matrix. Surface profile images in Fig. 5 demonstrate that in the absence of ZIS, random sized stacks of CNTs are unevenly distributed in the matrix of CNTs/PMMA whereas in the presence of ZIS, CNTs are homogeneously dispersed in the whole structure of PMMA matrix of ZIS-CNTs/PMMA composite, respectively. A similar observation is also found in XRD analysis.

Electrical conductivity

Electrical conductivity of the CNTs/PMMA and ZIS-CNTs/PMMA composites has been measured at 1 MHz for all synthesized composites with different filler loading and their plots are given at 1 MHz in Figs. 6(a) and 6(b), respectively. A tremendous increase in the values of conductivity was observed on the addition of small amount of CNTs and ZIS-

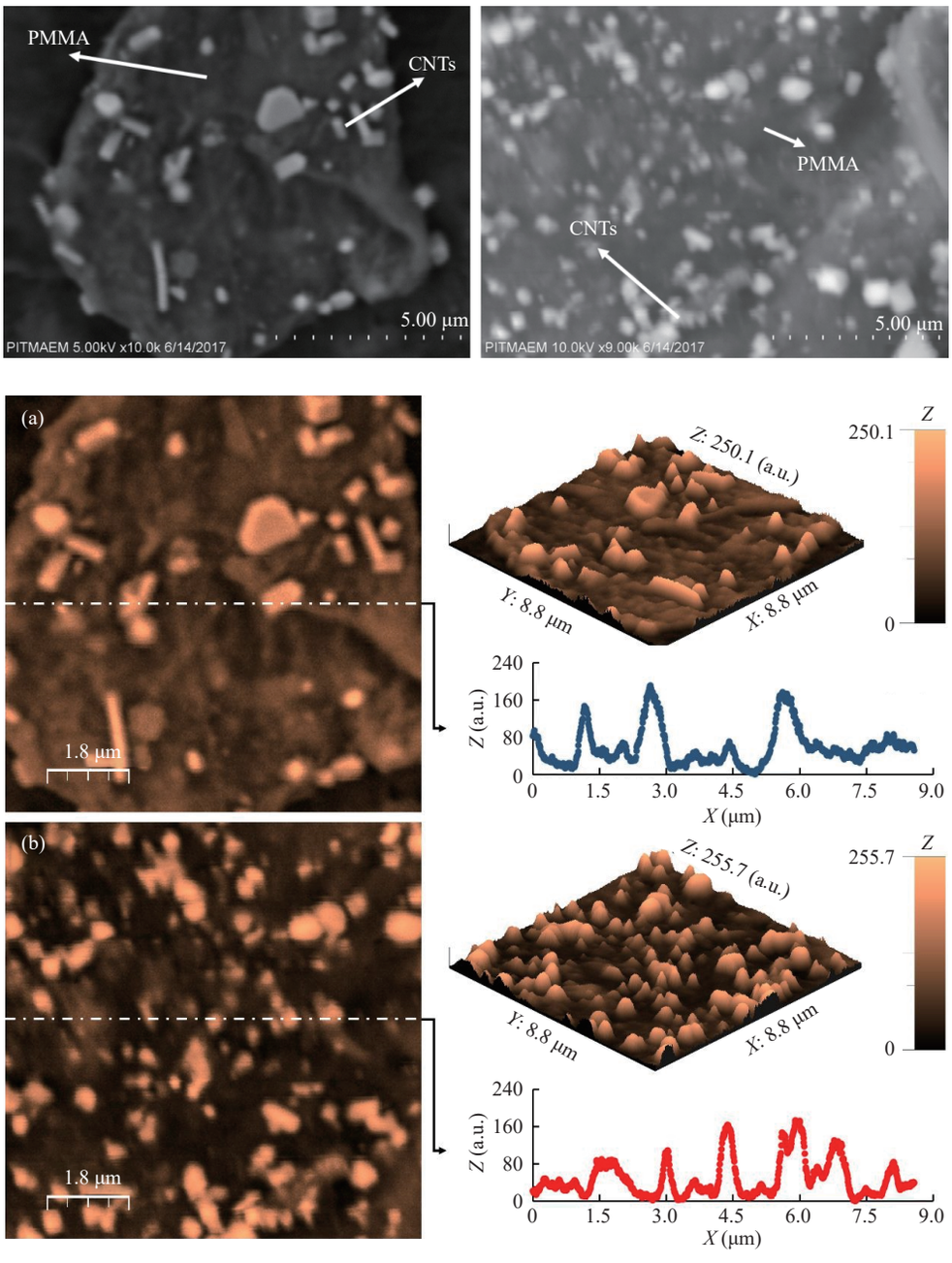

Fig. 5 SEM image of CNTs/PMMA composite (left) with surface profile of selected area and 3D micrograph as **(a)** and SEM image of ZIS-CNTs/PMMA composite (right) with surface profile of selected area and 3D micrograph as **(b)** at 10% of CNTs.

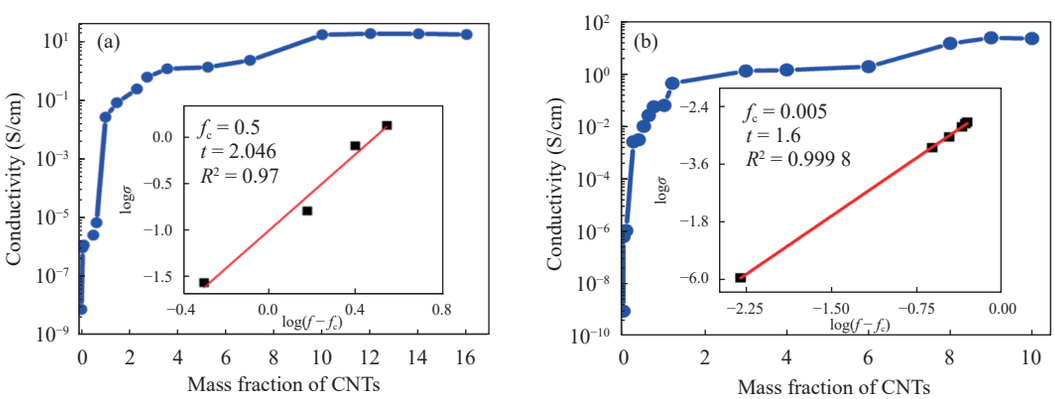

Fig. 6 Relation between the conductivity and different mass frations of CNTs in **(a)** CNTs/PMMA composites and **(b)** ZIS-CNTs/PMMA composites at 1 MHz.

CNTs. It can be observed that seven and eight order of magnitude increase in the conductivity was observed on addition of less than 1% of CNTs without and with ZIS, respectively. An almost 1 000 times increase in conductivity was observed around 0.05% and 0.0007% of CNTs without and with ZIS, respectively. Less than 100 times increase in conductivity has been reported on the addition of 0.2% of CNTs modified by maleic anhydride by Friedal–Craft acylation [30]. In another reported work [31], CNTs were dispersed in the solution with mechanical stirring followed by sonication for several hours for the formation of well dispersed and homogeneous CNTs/PMMA composites. Conductivity values obtained for these composites were 10^{-6} S/cm at 1%, 3.84×10^{-4} S/cm at 2%, and 10^{-2} S/cm at 3% of CNTs. In present work, the values of conductivity were observed in the range of 10^{-2} S/cm at only 1% and 0.5% of CNTs without and with ZIS, respectively. This increase is significant in comparison to reported values for similar systems [26, 32]. This significant increase in the value of the conductivity as compared to previously reported values is because of the uniform dispersion of the CNTs controlled by ZIS.

Reported values of percolation threshold and maximum conductivity along filler contents at which maximum conductivity was recorded for similar systems [5, 6, 32, 33] along the same values observed in the present case are given in Fig. 7 for comparison. The value of maximum conductivity is improved for synthesized CNTs/PMMA and ZIS-CNTs/PMMA composites as compared to reported values. Maximum conductivity values observed were 18 S/cm at 12% and 25 S/cm at 9% of filler contents for CNTs/PMMA and ZIS-CNTs/PMMA composites, respectively. While best values of maximum conductivity among the recently reported cases for the similar systems are 1.2 [32] and 0.01 S/cm [33], both at 3% CNTs. In these both cases, CNTs were modified by incorporating PMMA or polyethylene oxide (PEO) at their surface before synthesizing composites with PMMA. They aimed to develop the interaction between PMMA and CNTs through adsorbed PMMA or PEO at the surface of CNTs. This helped somehow in increasing the dispersion and thus improving the value of maximum conductivity. Since the dispersion of CNTs is very much sensitive towards the method of composite formation, modification, or pretreatment of CNTs and solvent used during the composite formation, in the present case, pretreatment of CNTs and modification of CNTs by adsorbing ZIS at their surface played a vital role in increasing the electrical conductivity. As the proposed role of ZIS in the introduction section, it is assumed that ZIS adsorbed at the surface of CNTs also made association with PMMA through its polar part. In this way, ZIS played a role in creating indirect interaction between CNTs and PMMA. It is reported that ZIS helped to disassemble the CNTs into individual tubes via electrostatic interaction by forming monolayers of ZIS onto the surfaces of CNTs [26, 34].

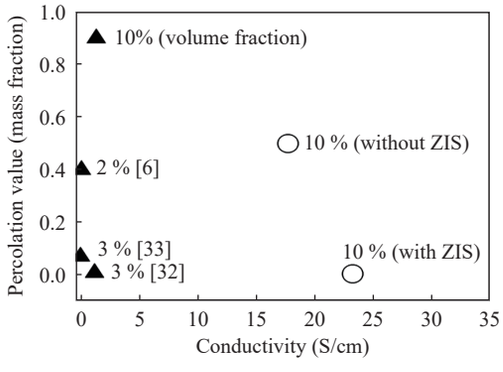

Fig. 7 Comparison of (▲) reported percolation threshold values along maximum conductivity observed at certain mass fration of CNTs for CNTs/PMMA composites with the same values from (O) present work.

Electrical properties of conducting filler-based polymer composites are best explained with the help of percolation models. The critical concentration of filler named percolation threshold, f_c, where the sudden rise in the conductivity of the composite is observed, is the key parameter of this model. The electrical percolation threshold of composites is well described by following the power law equation:

$$\sigma \alpha (f - f_c)^t, \quad \text{for} \quad f \geq f_c \tag{1}$$

where σ is the conductivity of the composites, f is the concentration of filler, f_c is the critical concentration at percolation, and t is the conductivity exponent. Values of f_c and t for both types of composites were determined by plotting linear fit log–log plot of power law given in Eq. (1). These linear plots for CNTs/PMMA and ZIS-CNTs/PMMA composites are shown in the insets of Figs. 6(a) and 6(b), respectively. Values of f_c and t determined for CNTs/PMMA composites are 0.5 and 2.05, and 0.005 and 1.6 for ZIS-CNTs/PMMA composites,

respectively. t values lie in the range reported for three-dimensional (3D) systems [35]. Recently, a research group working in this field [32] observed the percolation at 0.0095% which they were able to achieve by using CNTs-coated PMMA particles as fillers to synthesize composites with PMMA. Synthesis of the CNTs-coated PMMA particles involved a tedious experimental procedure. At another place [33], the value of the percolation threshold reported for similar systems is 0.07%. They claimed observation of low percolation threshold value with the help of PEO by adsorbing it at the surface of CNTs. They used 20% PEO for this purpose. In our case, the values of percolation threshold were observed at 0.005% and 0.5% for ZIS-CNTs/PMMA and CNTs/PMMA composites, respectively. As discussed above, in the case of ZIS-CNTs/PMMA, disassembling of CNTs and indirect interaction of CNTs with PMMA due to ZIS are the factors behind the homogeneous dispersion of CNTs which resulted in the observation of low percolation threshold.

Figures 8(a) and 8(b) depict the effect of frequency on the conductivity of CNTs/PMMA, and Figs. 8(c) and 8(d) show that of ZIS-CNTs/PMMA composites with different filler contents. It is observed that the extent of the effect of frequency is different not only for CNTs/PMMA from ZIS-CNTs/PMMA composites but also not the same for the same type of composites with different filler contents. For both types of composites, conductivity linearly increases with frequency for lower filler contents.

While for composites with higher CNTs contents, frequency-independent behavior is observed. This phenomenon can be well analyzed with the help of resistor–capacitor percolation model. According to that model, conductivity can be divided in two types. One of the types is the frequency-dependent, AC conductivity, and the other is frequency-independent, DC conductivity [36]. It is reported that polarization arises due to interfaces between conductive entities,

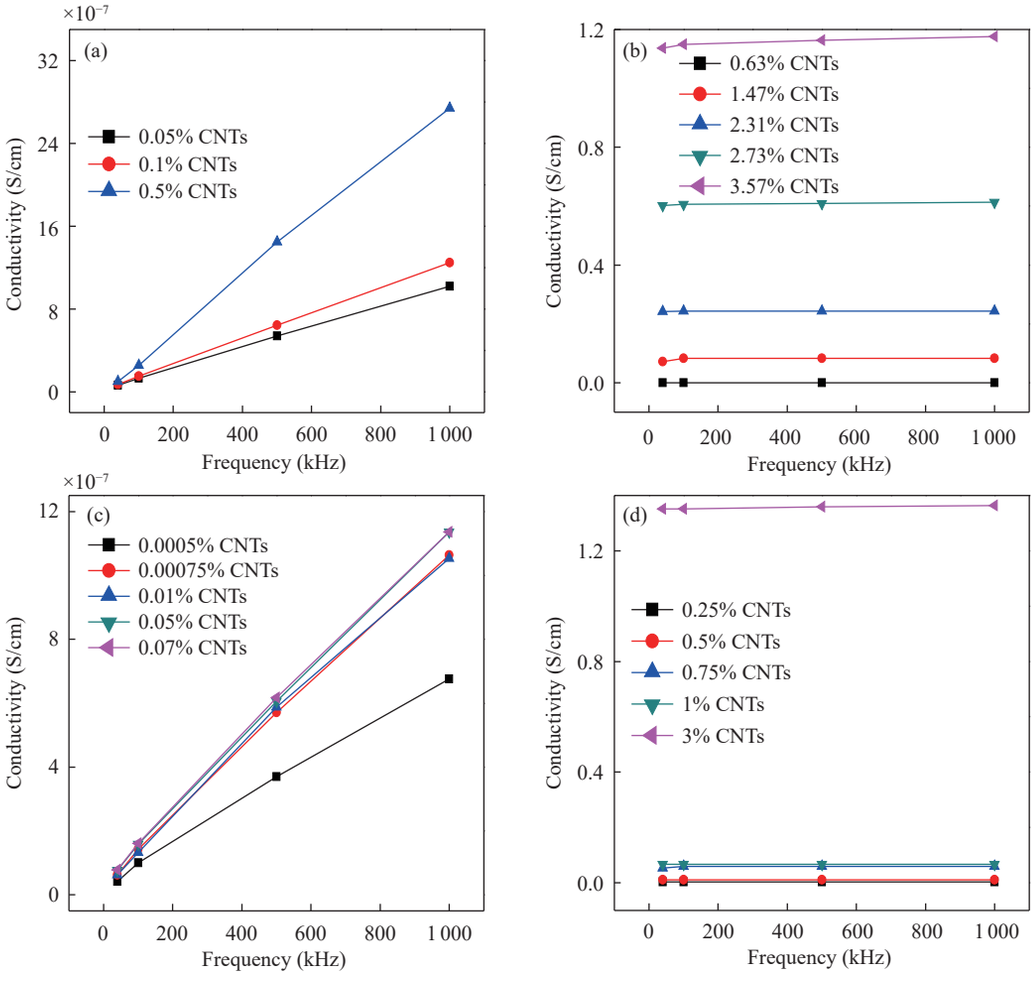

Fig. 8 Effect of frequency on conductivity for (**(a)** and **(b)**) CNTs/PMMA composites and (**(c)** and **(d)**) ZIS-CNTs/PMMA composites with different mass fractions of CNTs.

filler, and nonconductive regions, and matrix is the reason for this kind of frequency dependence conductivity provided no proper network exists as an alternative passage of current [37]. Due to this reason, AC conductivity, frequency-dependent conductivity is more pronounced at low filler contents where such interfaces exist. Basically, conductivity through this mechanism becomes more feasible at higher frequencies. While at higher filler contents, after the establishment of a proper conductive network, DC conductivity becomes pronounced where no facilitation from frequency is required anymore. It is also noticeable that transition filler contents and conversion of frequency dependence region to frequency independence region are lower for ZIS-CNTs/PMMA than CNTs/PMMA. This confirms our findings that ZIS helped in developing a conductive network at low filler loading by avoiding agglomeration.

Dielectric properties

Dielectric constant ε_r and dielectric loss ε were calculated by [38–40]:

$$\varepsilon_r = \frac{t_m C_p}{\pi\left(\frac{d}{2}\right)^2 \varepsilon} \tag{2}$$

$$\tan\delta = \frac{1}{2\pi f C_p R_p} \tag{3}$$

$$\varepsilon = \varepsilon_r \tan\delta \tag{4}$$

where t_m is the thickness of the sample, C_p is the capacitance in parallel, d is the diameter of the electrodes, ε_0 is the permittivity of free space (8.854×10^{-12} F/m), tanδ is the loss factor, R_p is the resistance in parallel, and f is the frequency. The dielectric constants for CNTs/PMMA and ZIS-CNTs/PMMA composites are given in Figs. 9(a) and 9(b) as a function of mass fraction of CNTs and Figs. 9(c) and 9(d) as a function of frequencies, respectively. From Figs. 9(a) and 9(b), it is witnessed that the dielectric constant values of both types of composites increase very rapidly upon the incorporation of CNTs. Almost 10 times increase is observed in the values of dielectric constant for ZIS-CNTs/PMMA at 0.25%, and 20 times for CNTs/PMMA at 1.5% CNTs as compared to the pure PMMA. The dielectric behavior of such kind of polymer composite is mainly due to the accumulation of charge at the interface of non conductive polymer and conductive filler. The value of the observed dielectric constant increases along the increase in the extent of interfacial surface area containing accumulated charge, due to an increase in conductive filler in insulator polymer until conductive network formation takes place. The maximum values of the dielectric constant observed are 23 at 1.47% and 12 at 0.37% CNTs for CNTs/PMMA and ZIS-CNTs/PMMA composites, respectively at 1 MHz. This trend is in accordance with the Maxwell–Wagner–Sillar effect [36, 41, 42]. Flipping of the dipole induced at the interface of filler and matrix is slow and adjustable at low frequency and thus. The dependence of dielectric constant on frequency is quite observable at lower frequency region as shown in Figs. 9(c) and 9(d). While at higher frequencies, reversal of the applied electric field is quite higher and dipoles are not able to attune themselves according to the frequency of the applied electric field. Thus, the value of dielectric constant remained ineffective when frequency change takes place in higher regions [43]. A similar kind of frequency response was also observed in Ref. [36].

Frequency dependence of dielectric loss for composites with different filler loadings is given in Figs. 9(e) and 9(f). As obvious, low values of dielectric loss are observed for both types of composites. It is reported that materials with such a low value of dielectric loss make them attractive for a number of applications such as actuators [44]. Here, it is evidenced by the frequency dependence response of dielectric loss that an increase in frequency helps in decreasing the extent of dielectric loss. This frequency dependence effect is more pronounced for ZIS-CNTs/PMMA composites than CNTs/PMMA while, in general, values of dielectric loss of CNTs/PMMA composites are lower than those of ZIS-CNTs/PMMA composites. As mentioned earlier, interfacial polarization between CNTs is reduced due to the additional ZIS and causes reduction in reagglomeration. Similarly, ZIS is also responsible for the increase in the dielectric loss due to the presence of polar functional group (hydrophilic-sulfonate with a quaternary ammonium head group) that not only absorbs the electromagnetic energy but also causes the interfacial polarization which results in the increase in dielectric loss. However, in CNT/PMMA composites, these polar groups are absent; therefore, its dielectric loss is comparatively low. One more reason for this difference is the direct association of dielectric loss to conductivity. In

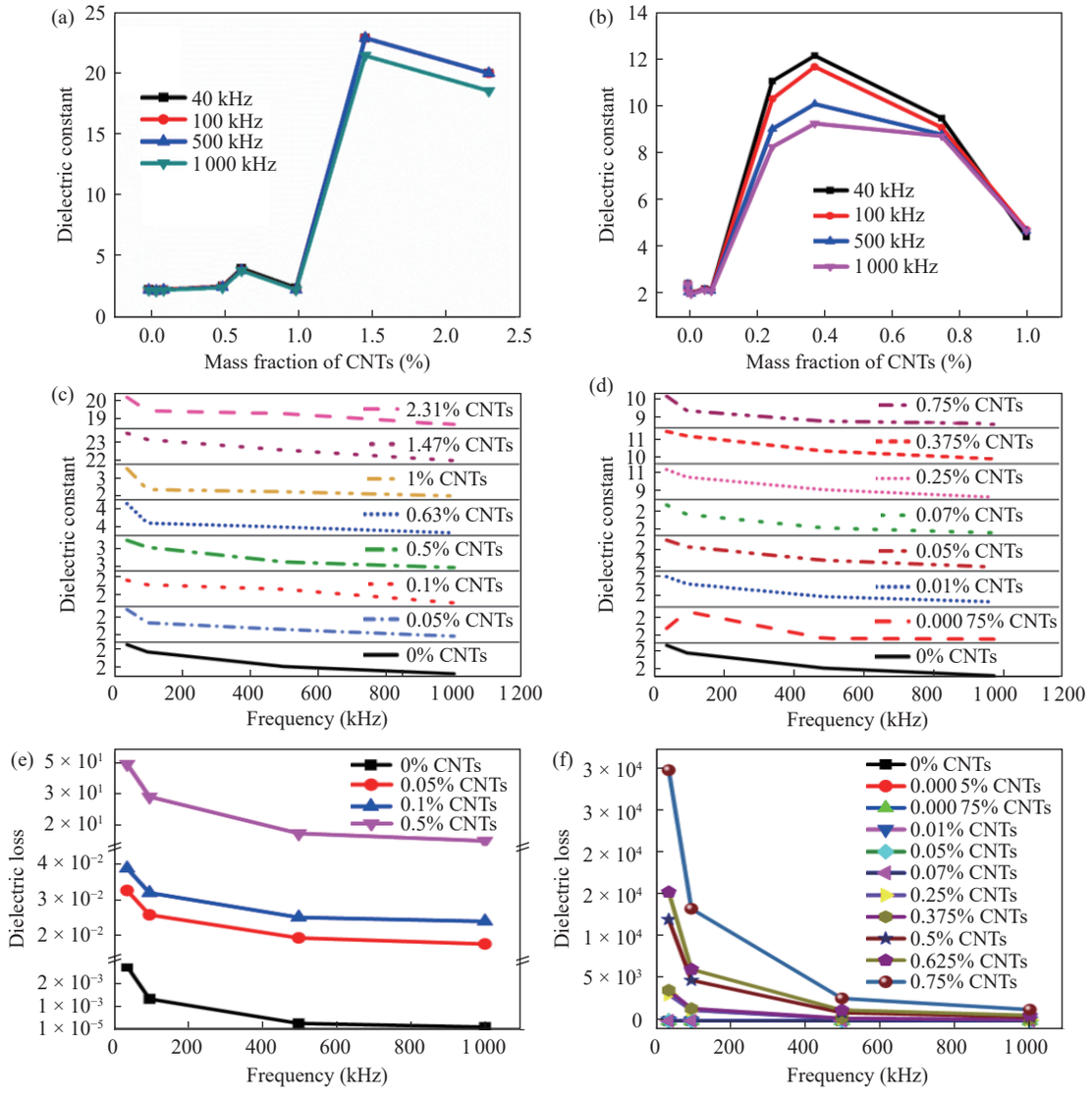

Fig. 9 Comparison of dielectric constant with respect to (**(a)** and **(b)**) mass fration of CNTs, and with respect to (**(c)** and **(d)**) frequency and (**(e)** and **(f)**) dielectric loss of CNTs /PMMA and ZIS-CNTs/PMMA composites, respectively.

present research, percolation threshold was achieved at far lower loading for ZIS-CNTs/PMMA as compared to CNTs/PMMA composites. Conductivity was also relatively high for ZIS-CNTs/PMMA; therefore, the value of dielectric loss is also higher for ZIS-CNTs/PMMA composites than for CNTs/PMMA. Comparison of conducting and dielectric properties of CNTs/PMMA and ZIS-CNTs/PMMA composites is elaborated in Table 2 as follows.

Thermal properties

Results obtained by TGA analysis of PMMA, CNTs/PMMA, and ZIS-CNTs/PMMA composites at 10% CNTs are shown in Fig. 10 and these results show that ZIS helped in increasing the thermal stability of the composites. It is observed that the CNTs/PMMA and ZIS-CNTs/PMMA composites show a better thermal stability as compared to pure PMMA, and similar findings are also observed for such polymer composites in Refs. [45, 46].

Table 2 Summary of the conducting and dielectric properties of CNTs/PMMA and ZIS-CNTs/PMMA composites

Composite	Conductivity (S/cm)	Percolation threshold (f_c)	Dielectric constant	Dielectric loss at 0.5%
CNTs/PMMA	18 (12%)	0.5	2.7 (0.5%), 23 (1.47%)*	5.4×10^1
ZIS-CNTs/PMMA	25 (9%)	0.005	12 (0.37%)*	1.2×10^4

*shows maximum value.

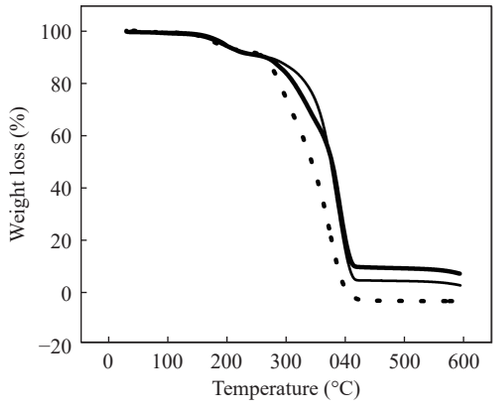

Fig. 10 TGA analysis of PMMA (dotted), CNTs/PMMA (thin line), and ZIS-CNTs/PMMA (thick line) composites at 10% CNTs.

Two-step degradation of PMMA as reported in Refs. [47–49] and in CNTs/PMMA composite is also present in ZIS-CNTs/PMMA composite with improved thermal stability. Though vinyl PMMA end group [50] started degradation from 150 to 225 °C for ZIS-CNTs/PMMA composite, the random scission region that started degradation from 225 °C continued till 590 °C with still 7% of the remaining mass.

As reported in different PMMA composites, the thermal stability could be determined by the increment in char yield [51, 52]. An increase in char yield of ZIS-CNTs/PMMA composite witnessed the improvement in the thermal stability of PMMA. A detail of weight loss with respect to temperature is shown in Table 3 along with the char yield percentage which shows the residue left at the end of the TGA analysis.

The reason for the better stability of ZIS-CNTs/PMMA than CNTs/PMMA is because of the establishment of an indirect association between CNTs and PMMA through ZIS. This assumption is in line with the results obtained through the measurement of electrical properties, decrease in the optical band gap, XRD patterns, and SEM images. Overall, the maximum mass loss of the synthesized composites seems to be quite convincing when compared to data reported in the literature for similar systems [53, 54].

Table 3 Temperature weight loss summary for PMMA and its composites with CNTs and ZIS-CNTs at 10% filler

Sample ID	Decomposition start (°C)	Decomposition mid (°C)	Decomposition end (°C)	Char yield at 593 °C (%)
PMMA	29.87	330.4	600	0.34
CNTs/PMMA	36.845	376.233	593.4	2.67
ZIS-CNTs/PMMA	29.6	376.23	593	7

Conclusion

A series of percolative conductive composites of PMMA matrix, with CNTs and ZIS-CNTs as filler, were synthesized by solution casting method. FTIR and UV–Vis spectroscopy confirmed the successful synthesis of the composites. SEM and XRD studies revealed that modified CNTs by ZIS were more effectively dispersed than pristine CNTs. A low value of the percolation threshold and high value of maximum conductivity demonstrated that modification of CNTs by ZIS was significantly encouraging. The decrease in the optical band gap from 4.31 (PMMA) to 3.7 eV (CNTs/PMMA) and further reduction to 3.08 eV (ZIS-CNTs/PMMA composites) supported the increase in the electrical conductivity of the composites. Thermal stabilities of the composites were enhanced than pure PMMA. As compared to the literature, improved electrical properties with the lowest percolation threshold and better thermal stability have been obtained for ZIS-CNTs/PMMA composites.

CRediT Author Statement

Farrukh Bashir and **Tajamal Hussain**: Conceptualization, investigation, methodology, supervision, analysis and writing. **Adnan Mujahid, Mirza Nadeem Ahmad, Muhammad Zahid, Muhammad Imran Din, Ayesha Mushtaq** and **Huma Tareen:** Draft editing, review, and analysis. **Muhammad Aamir Raza:** Characterization.

Acknowledgment

The authors are greatful to Dr. Zulfiqar Ali, Chairman/associate professor, Department of Mining Engineering, University of Engineering Technology, Lahore, Pakistan, and Engineer Muhammad Irfan, Head of Pakistan Institute of Technology for Minerals & Advanced Engineering Materials (PITMAEM), and Dr. Saqib Nasir, Senior Scientific Officer, Pakistan Council of Scientific and Industrial Research Laboratories, Complex, Lahore, Pakistan for

technical support. The authors acknowledge the University of Punjab, Lahore, for financial support to carry out this research work through a research project (PU Research Grant 2017-18).

Conflict of Interest

All authors have no conflict of interest.

References

[1] J. Chen, Y. Zhu, J. Huang, et al. Advances in responsively conductive polymer composites and sensing applications. *Polymer Reviews*, 2021, 61(1): 157−193. https://doi.org/10.1080/15583724.2020.1734818

[2] Z. Spitalsky, D. Tasis, K. Papagelis, et al. Carbon nanotube–polymer composites: chemistry, processing, mechanical and electrical properties. *Progress in Polymer Science*, 2010, 35(3): 357−401. https://doi.org/10.1016/j.progpolymsci.2009.09.003

[3] K. Shehzad, T. Hussain, A.T. Shah, et al. Effect of the carbon nanotube size dispersity on the electrical properties and pressure sensing of the polymer composites. *Journal of Materials Science*, 2016, 51(24): 11014−11020. https://doi.org/10.1007/s10853-016-0322-9

[4] K. Mosnáčková, Z. Špitálský, J. Kuliček, et al. Influence of preparation methods on the electrical and nanomechanical properties of poly(methyl methacrylate)/multiwalled carbon nanotubes composites. *Journal of Applied Polymer Science*, 2015, 132(13): 41721. https://doi.org/10.1002/app.41721

[5] R. Patra, S. Suin, D. Mandal, et al. Sequential mixing as effective method in the reduction of percolation threshold of multiwall carbon nanotube in poly(methyl methacrylate)/high-density poly(ethylene)/MWCNT nanocomposites. *Journal of Applied Polymer Science*, 2014, 131(10): 40235. https://doi.org/10.1002/app.40235

[6] A. Kumar, K. Sharma, A.R. Dixit. A review on the mechanical properties of polymer composites reinforced by carbon nanotubes and graphene. *Carbon letters*, 2021, 31(2): 149−165. https://doi.org/10.1007/s42823-020-00161-x

[7] T. Hussain, F. Bashir, A. Mujahid, et al. Highly stable APTES incorporated CNTs based ternary polymer composites with improved dielectric and thermal properties. *Silicon*, 2022, 14: 10807−10816. https://doi.org/10.1007/s12633-022-01782-9

[8] F. Bashir, T. Hussain, A. Mujahid, et al. Tailoring electrical and thermal properties of polymethyl methacrylate-carbon nanotubes composites through polyaniline and dodecyl benzene sulphonic acid impregnation. *Polymer Composites*, 2018, 39(S2): E1052−E1059. https://doi.org/10.1002/pc.24485

[9] N. Mohd Nurazzi, M.R.M. Asyraf, A. Khalina, et al. Fabrication, functionalization, and application of carbon nanotube-reinforced polymer composite: An overview. *Polymers*, 2021, 13(7): 1047. https://doi.org/10.3390/polym13071047

[10] B. Fugetsu, W. Han, N. Endo, et al. Disassembling single-walled carbon nanotube bundles by dipole/dipole electrostatic interactions. *Chemistry Letters*, 2005, 34(9): 1218−1219. https://doi.org/10.1246/cl.2005.1218

[11] R. Yadav, K. Kumar, P. Venkatesu. Covalent functionalization of carbon nanotube. In: Handbook of Carbon Nanotubes. Cham: Springer, 2021: 1–28. https://doi.org/10.1007/978-3-319-70614-6_65-1

[12] R.J. Chen, Y. Zhang, D. Wang, et al. Noncovalent sidewall functionalization of single-walled carbon nanotubes for protein immobilization. *Journal of the American Chemical Society*, 2001, 123(16): 3838−3839. https://doi.org/10.1021/ja010172b

[13] M.J. O'Connell, P. Boul, L.M. Ericson, et al. Reversible water-solubilization of single-walled carbon nanotubes by polymer wrapping. *Chemical Physics Letters*, 2001, 342(3/4): 265–271. https://doi.org/10.1016/S0009-2614(01)00490-0

[14] H. Tajamal, M. Tayyaba, M. Adnan, et al. Polystyrene adsorbed multi-walled carbon nanotubes incorporated polymethylmethacrylate composites with modified percolation phenomena. *MRS Advances*, 2018, 3(1/2): 25–30. https://doi.org/10.1557/adv.2017.625

[15] B.J. Sanghavi, A.K. Srivastava, Simultaneous voltammetric determination of acetaminophen, aspirin and caffeine using an *in situ* surfactant-modified multiwalled carbon nanotube paste electrode. *Electrochimica Acta*, 2010, 55(28): 8638–8648. https://doi.org/10.1016/j.electacta.2010.07.093

[16] Ö. Güler, N.N. Cacim, E. Evin, et al. The synergistic effect of CNTs-polymeric surfactant on the properties of concrete nanocomposites: Comparative study. *Journal of Composite Materials*, 2021, 55(10): 1371−1384. https://doi.org/10.1177/0021998320971346

[17] J. Parameswaranpillai, G. Joseph, S.K. Sidhardhan, et al. Miscibility, UV resistance, thermal degradation, and mechanical properties of PMMA/SAN blends and their composites with MWCNTs. *Journal of Applied Polymer Science*, 2016, 133(30): 43628. https://doi.org/10.1002/app.43628

[18] R. Sarkar, A. Pal, A. Rakshit, et al. Properties and applications of amphoteric surfactant: A concise review. *Journal of Surfactants and Detergents*, 2021, 24(5): 709−730. https://doi.org/10.1002/jsde.12542

[19] Z. Wang, Q. Liu, H. Zhu, et al. Dispersing multi-walled carbon nanotubes with water–soluble block copolymers and their use as supports for metal nanoparticles. *Carbon*, 2007, 45(2): 285−292. https://doi.org/10.1016/j.carbon.2006.09.025

[20] J.D. Hartgerink, E. Beniash, S.I. Stupp. Self-assembly and mineralization of peptide-amphiphile nanofibers. *Science*, 2001, 294(5547): 1684−1688. https://doi.org/10.1126/science.1063187

[21] J. Vilčáková, R. Moučka, P. Svoboda, et al. Effect of surfactants and manufacturing methods on the electrical and thermal conductivity of carbon nanotube/silicone composites. *Molecules*, 2012, 17(11): 13157−13174. https://doi.org/10.3390/molecules171113157

[22] A. Tomar, S. Mahendia, S. Kumar. Structural characterization of PMMA blended with chemically synthesized PAni. *Advances in Applied Science Research*, 2011, 2(3): 327−333.

[23] L. Lavagna, D. Massella, M. Pavese. Preparation of hierarchical material by chemical grafting of carbon nanotubes onto carbon fibers. *Diamond and Related*

Materials, 2017, 80: 118−124. https://doi.org/10.1016/j.diamond.2017.10.013

[24] R. Kumar, S.A. Ali, P. Singh, et al. Physical and chemical response of 145 MeV Ne^{6+} ion irradiated polymethylmethacrylate (PMMA) polymer. *Nuclear Instruments and Methods in Physics Research Section B*: *Beam Interactions With Materials and Atoms*, 2011, 269(14): 1755−1759. https://doi.org/10.1016/j.nimb.2010.12.025

[25] R.B. Viana, A.B.F. Da Silva, A.S. Pimentel. Infrared spectroscopy of anionic, cationic, and zwitterionic surfactants. *Advances in Physical Chemistry*, 2012, 2012: 903272. https://doi.org/10.1155/2012/903272

[26] H.N. Najeeb, A.A. Balakit, G.A. Wahab, et al. Study of the optical properties of poly(methyl methaacrylate) (PMMA) doped with a new diarylethen compound. *Academic Research International*, 2014, 5(1): 48−56.

[27] U. Jabeen, S.M. Shah, N. Hussain, et al. Synthesis, characterization, band gap tuning and applications of Cd-doped ZnS nanoparticles in hybrid solar cells. *Journal of Photochemistry and Photobiology A*: *Chemistry*, 2016, 325: 29−38. https://doi.org/10.1016/j.jphotochem.2016.04.003

[28] J. Al-Osaimi, N.M. Al-Hosiny, A. Badawi, et al. The effects of CNTs types on the structural and electrical properties of CNTs/PMMA nanocomposite films. *International Journal of Engineering & Technology*, 2013, 13(2): 77−79.

[29] X. Yao, H. Wu, J. Wang, et al. Carbon nanotube/poly(methyl methacrylate)(CNT/PMMA) composite electrode fabricated by in situ polymerization for microchip capillary electrophoresis. *Chemistry–A European Journal*, 2007, 13(3): 846−853. https://doi.org/10.1002/chem.200600469

[30] Y.-L. Huang, S.-M. Yuen, C.-C.M. Ma, et al. Morphological, electrical, electromagnetic interference (EMI) shielding, and tribological properties of functionalized multi-walled carbon nanotube/poly methyl methacrylate (PMMA) composites. *Composites Science and Technology*, 2009, 69(11/12): 1991–1996. https://doi.org/10.1016/j.compscitech.2009.05.006

[31] D.O. Kim, M.H. Lee, J.H. Lee, et al. Transparent flexible conductor of poly(methyl methacrylate) containing highly-dispersed multiwalled carbon nanotube. *Organic Electronics*, 2008, 9(1): 1−13. https://doi.org/10.1016/j.orgel.2007.07.004

[32] S.H. Ryu, H.-B. Cho, J.W. Moon, et al. Highly conductive polymethly (methacrylate)/multi-wall carbon nanotube composites by modeling a three-dimensional percolated microstructure. *Composites Part A*: *Applied Science and Manufacturing*, 2016, 91: 133−139. https://doi.org/10.1016/j.compositesa.2016.10.002

[33] S.M. Mir, S.H. Jafari, H.A. Khonakdar, et al. A promising approach to low electrical percolation threshold in PMMA nanocomposites by using MWCNT-PEO predispersions. *Materials & Design*, 2016, 111: 253−262. https://doi.org/10.1016/j.matdes.2016.08.073

[34] J. Nguyen, H. Wen, Z. Zhang, et al. Surfactant assisted dispersion and adhesion behavior of carbon nanotubes on Cu–Zr and Cu–Zr–Al amorphous powders. *Journal of Materials Science & Technology*, 2014, 30(9): 847−853. https://doi.org/10.1016/j.jmst.2014.07.002

[35] Z.-M. Dang, K. Shehzad, J.-W. Zha, et al. On refining the relationship between aspect ratio and percolation threshold of practical carbon nanotubes/polymer nanocomposites. *Japanese Journal of Applied Physics*, 2011, 50(8R): 080214. https://doi.org/10.1143/JJAP.50.080214

[36] K. Shehzad, Z.-M. Dang, M.N. Ahmad, et al. Effects of carbon nanotubes aspect ratio on the qualitative and quantitative aspects of frequency response of electrical conductivity and dielectric permittivity in the carbon nanotube/polymer composites. *Carbon*, 2013, 54: 105−112. https://doi.org/10.1016/j.carbon.2012.10.068

[37] N.J.S. Sohi, S. Bhadra, D. Khastgir. The effect of different carbon fillers on the electrical conductivity of ethylene vinyl acetate copolymer-based composites and the applicability of different conductivity models. *Carbon*, 2011, 49(4): 1349−1361. https://doi.org/10.1016/j.carbon.2010.12.001

[38] B. Sannakki, Anita. Dielectric properties of PMMA and its composites with ZrO_2. *Physics Procedia*, 2013, 49: 15−26. https://doi.org/10.1016/j.phpro.2013.10.006

[39] S. Islam, G.B.V.S. Lakshmi, A.M. Siddiqui, et al. Synthesis, electrical conductivity, and dielectric behavior of polyaniline/V_2O_5 composites. *International Journal of Polymer Science*, 2013, 2013: 307525. https://doi.org/10.1155/2013/307525

[40] H.-Y. Mi, Z. Li, L.-S. Turng, et al. Silver nanowire/thermoplastic polyurethane elastomer nanocomposites: Thermal, mechanical, and dielectric properties. *Materials & Design*, 2014, 56: 398–404. https://doi.org/10.1016/j.matdes.2013.11.029

[41] E. Lim, T. Manaka, R. Tamura, et al. Maxwell–Wagner model analysis for the capacitance–voltage characteristics of pentacene field effect transistor. *Japanese Journal of Applied Physics*, 2006, 45(4S): 3712. https://doi.org/10.1143/JJAP.45.3712

[42] G. Zou, E. Lim, R. Tamura, et al. Surface morphology and electrical transport properties of polydiacetylene-based organic field-effect transistors. *Japanese Journal of Applied Physics*, 2006, 45(8R): 6436. https://doi.org/10.1143/JJAP.45.6436

[43] I. Tantis, D. Tasis, G. Psarras. Functionalized graphene-poly (vinyl alcohol) nanocomposites: Physical and dielectric properties. *eXPRESS Polymer Letters*, 2012, 6(4): 283−292. https://doi.org/10.3144/expresspolymlett.2012.31

[44] Z.H. Li, S.Y. Chen, S. Nambiar, et al. PMMA/MWCNT nanocomposite for proton radiation shielding applications. *Nanotechnology*, 2016, 27(23): 234001. https://doi.org/10.1088/0957-4484/27/23/234001

[45] R. Pelrine, P. Sommer-Larsen, R.D. Kornbluh, et al. Applications of dielectric elastomer actuators. In: Proceedings of the SPIE's 8th Annual International Symposium on Smart Structures and Materials: Electroactive Polymer Actuators and Devices, 2001, 4329: 335–349. https://doi.org/10.1117/12.432665

[46] J.F. Dai, Q. Wang, W.X. Li, et al. Properties of well aligned SWNT modified poly(methyl methacrylate) nanocomposites. *Materials Letters*, 2007, 61(1): 27−29. https://doi.org/10.1016/j.matlet.2006.03.156

[47] Y.-H. Hu, C.-Y. Chen. The effect of end groups on the thermal degradation of poly(methyl methacrylate). *Polymer Degradation and Stability*, 2003, 82(1): 81−88.

https://doi.org/10.1016/S0141-3910(03)00165-4

[48] J.D. Peterson, S. Vyazovkin, C.A. Wight. Stabilizing effect of oxygen on thermal degradation of poly(methyl methacrylate). *Macromolecular Rapid Communications*, 1999, 20(9): 480−483. https://doi.org/10.1002/(SICI)1521-3927(19990901)20:9<480::AID-MARC480>3.0.CO;2-7

[49] N. Grassie. C.—Degradation. The mechanism of the thermal degradation of polymethyl methacrylate. *Discussions of the Faraday Society*, 1947, 2(1): 378−383. https://doi.org/10.1039/DF9470200378

[50] T. Kashiwagi, A. Inaba, J.E. Brown, et al. Effects of weak linkages on the thermal and oxidative degradation of poly(methyl methacrylates). *Macromolecules*, 1986, 19(8): 2160−2168. https://doi.org/10.1021/ma00162a010

[51] S. Rahimi-Razin, V. Haddadi-Asl, M. Salami-Kalajahi, et al. Properties of matrix-grafted multi-walled carbon nanotube/poly(methyl methacrylate) nanocomposites synthesized by in situ reversible addition-fragmentation chain transfer polymerization. *Journal of the Iranian Chemical Society*, 2012, 9(6): 877−887. https://doi.org/10.1007/s13738-012-0104-5

[52] S.N. Tripathi, P. Saini, D. Gupta, et al. Electrical and mechanical properties of PMMA/reduced graphene oxide nanocomposites prepared via in situ polymerization. *Journal of Materials Science*, 2013, 48(18): 6223−6232. https://doi.org/10.1007/s10853-013-7420-8

[53] S. Kumar, T. Rath, B.B. Khatua, et al. Preparation and characterization of poly(methyl methacrylate)/multi-walled carbon nanotube composites. *Journal of Nanoscience and Nanotechnology*, 2009, 9(8): 4644−4655. https://doi.org/10.1166/jnn.2009.220

[54] Y.-H. Hu, C.-Y. Chen, C.-C. Wang. Viscoelastic properties and thermal degradation kinetics of silica/PMMA nanocomposites. *Polymer Degradation and Stability*, 2004, 84(3): 545−553. https://doi.org/10.1016/j.polymdegradstab.2004.02.001